Ultrafast molecular orbital tomography of a pentacene thin film using time-resolved momentum microscopy at a free-electron laser

M. Scholz,[1,*] K. Baumgärtner,[2] C. Metzger,[2] D. Kutnyakhov,[3] M. Heber,[3] F. Pressacco,[3] C.H. Min,[4] T.R.F. Peixoto,[2] M. Reiser,[1] C. Kim,[1] W. Lu,[1] R. Shayduk,[1] W. M. Izquierdo,[1] G. Brenner,[3] F. Roth,[5] A. Schöll,[2] S. Molodtsov,[1,5] W. Wurth†,[3,6,7] F. Reinert,[2] and A. Madsen[1]

[1]*European X-Ray Free-Electron Laser Facility, Holzkoppel 4, 22869 Schenefeld, Germany*

[2]*Experimentelle Physik 7, Julius-Maximilians-Universität, Am Hubland, 97074 Würzburg, Germany*

[3]*Deutsches Elektronen-Synchrotron DESY, Notkestrasse 85, 22607 Hamburg, Germany*

[4]*Institut für Experimentelle und Angewandte Physik, Christian-Albrechts-Universität zu Kiel, 24098 Kiel, Germany*

[5]*Institute of Experimental Physics, TU Bergakademie Freiberg, Leipziger Strasse 23, 09599 Freiberg, Germany*

[6]*The Hamburg Centre for Ultrafast Imaging (CUI), Luruper Chaussee 149, 22761 Hamburg, Germany*

[7]*Department Physik and Centre for Free-Electron Laser Science, Universität Hamburg, Luruper Chaussee 149, 22761 Hamburg, Germany*

SAMPLE PREPARATION AND ENERGY CALIBRATION

For every film preparation we checked the film quality and thickness by low-energy electron diffraction (LEED). The first layer of pentacene on Ag(110) exhibits a characteristic pattern that is distinguishable from the second and subsequent layers [1, 2]. Fig. 1 a) shows a typical LEED pattern of a bilayer of pentacene atop Ag(110).

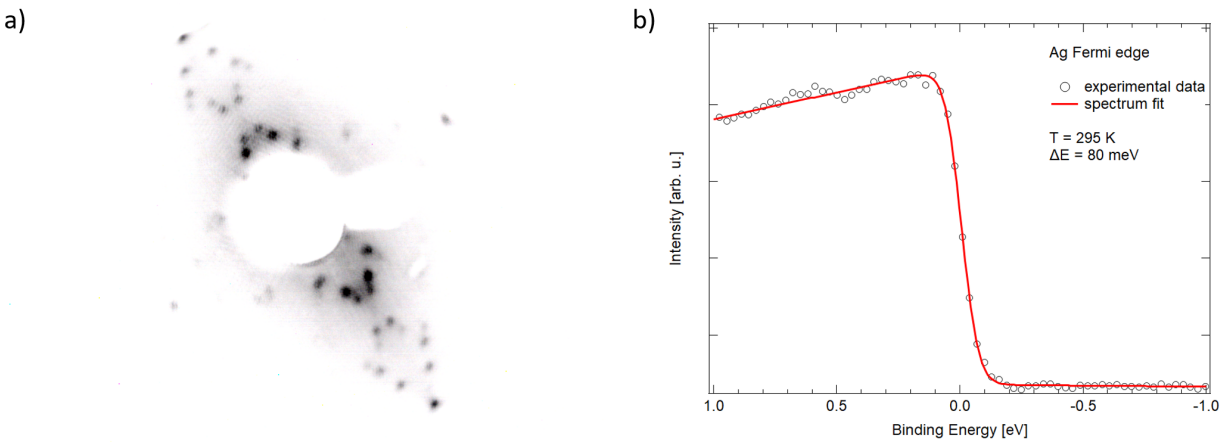

Figure 1: a) LEED pattern of pentacene bilayer on Ag(110) for an electron energy of 30 eV. b) Fermi edge of Ag single crystal at 295 K. From fitting the Fermi edge we determine an energy resolution of about 80 meV (Fig. 1 b)).

The momentum microscope was energy calibrated at the Fermi edge of a Ag single crystal at 295 K. The instrumental energy resolution was determined by fitting the Fermi edge of Ag and considering the temperature. From the fit parameters, we estimate an energy resolution of about 80 meV.

PHOTOEMISSION SIMULATION

The photoemission simulations are based on DFT calculations of an isolated pentacene molecule using Gaussian 09W [3] with a 6-31G+ basis set. We employ the linear combination of atomic orbitals (LCAO) and the B3LYP functional [4, 5] to quantify the matrix elements of Fermi's Golden Rule with final states in the independent atomic center approximation (IAC). This one-step model

of photoemission is similar to methods already detailed in literature [2, 6–8]. The photoemission intensity $I_n(\vec{k})$ at wavevector $\vec{k}$ of a molecular orbital n is constructed from the coherent superposition of all atomic contributions:

$$I_n(\vec{k}) \propto \left| \sum_a \left\langle \psi_{i,a} | \vec{\epsilon} \cdot \vec{r} | \psi_{f,a}(\vec{k}) \right\rangle \right|^2 \tag{1}$$

with the interaction operator $\vec{\epsilon} \cdot \vec{r}$ of the incoming electromagnetic field and the partial initial and final states $\psi_{i,a}$ and $\psi_{f,a}$ at atom a.
Similarly, the final state is the coherent superposition of partial final states $\psi_{f,a}$ at each atomic site a

$$\psi_{f,a} \; = \; 4\pi \sum_{l=0}^{\infty} \sum_{m=-l}^{l} (-1)^l j_l(kr) Y_{l,m}(\hat{r}) Y^*_{l,m}(\hat{k}) D_a(k) \delta^l_a(k) e^{-i\vec{k}\cdot\vec{R}_a} \tag{2}$$

with spherical Bessel functions j_l, spherical harmonics $Y_{l,m}$, inelastic damping D_a and phase shift δ^l_a from the potential of the emitting atom a. The interaction operator is taken from the known geometry and light polarization in the experiment.

Fig. 2 displays the thus calculated initial states and the PMM based thereon for the pentacene LUMO (top row) and HOMO (bottom row). For a two layer pentacene film on Ag(110), a mirror domain with a tilt around the long molecular axis was reported [2]. Subsequently, the PMM is the superposition of calculations for both tilt angles, e.g. -6.0 ° (f) and +6.0 °, around the long molecular axis of isolated molecules.

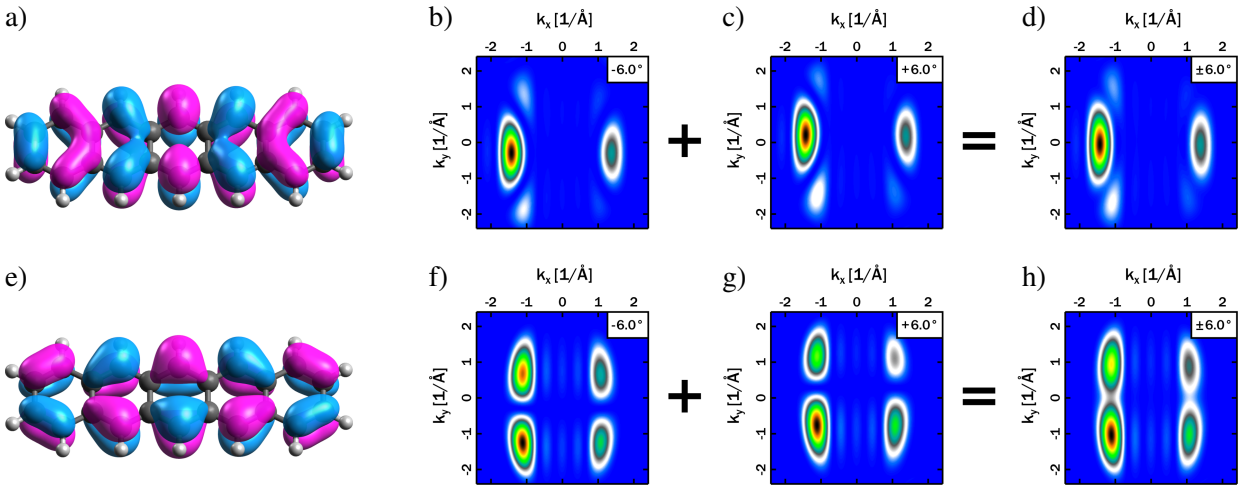

Figure 2: (a) Pentacene LUMO calculated with DFT for an isolated molecule. The simulated PMM under excitation conditions identical to the experiment for molecules rotated around the long molecular axis by -6.0 ° (b), +6.0 ° (c), as well as their superposition (d) are shown in the top row. Analogously, the bottom row displays the calculated pentacene HOMO (e), the PMM for rotations of -6.0 ° (f) and +6.0 ° (g) as well as their superposition (h).

ERROR ESTIMATION

The $1\,\sigma$ error-bars of the momentum distribution curves are estimated by two procedures. Firstly, we determine the intensity fluctuation within a region of interest (ROI) in the PMMs. In Fig. 4 the ROI (white rectangular) is exemplary shown for $\mathrm{LUMO}_{1\mathrm{st}}$ (left), $\mathrm{HOMO}_{1\mathrm{st}}$ (middle) and $\mathrm{HOMO}_{2\mathrm{nd}}$ (right) for $\tau_{\mathrm{Delay}} = $ -500 fs. The ROI does not contain any signal originating directly from the molecular orbitals, as shown by the simulations of the free molecule. We assume that the intensity is constant within the ROI and over time. Thus, we estimated an experimental error from the intensity fluctuation. Secondly, we compare the momentum distributions at two time steps before time zero ($\tau_{\mathrm{Delay}} = $ -500 fs and $\tau_{\mathrm{Delay}} = $ -150 fs). Therefore, we analyze five linecuts along the direction in momentum space, marked by the green dashed lines in Fig. 4. The $1\,\sigma$ error-bars is then calculated as the mean of the both errors.

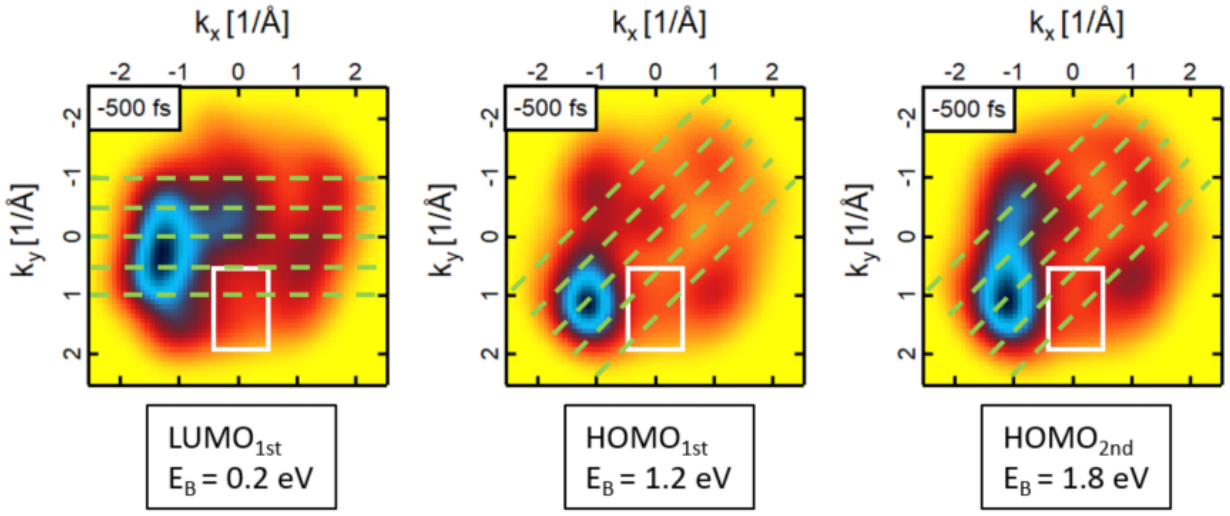

Figure 3: Time-resolved photoelectron momentum mapps (PMMs) of Pentacene of the $\mathrm{LUMO_{1st}}$ (left), $\mathrm{HOMO_{1st}}$ (middle) and $\mathrm{HOMO_{2nd}}$ (right). The green dashed lines the and the white rectangular areas in the PMMs indicate, where the errors were estimated.

---

* To whom correspondence should be addressed; E-mail:markus.scholz@xfel.eu.

[1] Y. L. Wang, W. Ji, D. X. Shi, S. X. Du, C. Seidel, Y. G. Ma, H.-J. Gao, L. F. Chi, and H. Fuchs, Structural evolution of pentacene on a Ag(110) surface, Physical Review B **69**, 10.1103/PhysRevB.69.075408 (2004).

[2] M. Grimm, C. Metzger, M. Graus, M. Jugovac, G. Zamborlini, V. Feyer, A. Schöll, and F. Reinert, Molecular orbital imaging beyond the first monolayer: Insights into the pentacene/Ag(110) interface, Physical Review B **98**, 195412 (2018).

[3] M. J. Frisch, G. W. Trucks, H. B. Schlegel, G. E. Scuseria, M. A. Robb, J. R. Cheeseman, G. Scalmani, V. Barone, and B. Mennucci, Gaussian Inc., Wallingford, CT, Gaussian 09 (Revision-A. 02), Inc., Wallingford, CT **4** (2009).

[4] A. D. Becke, A new mixing of Hartree–Fock and local density-functional theories, The Journal of Chemical Physics **98**, 1372 (1993).

[5] C. Lee, W. Yang, and R. G. Parr, Development of the Colle-Salvetti correlation-energy formula into a functional of the electron density, Physical Review B **37**, 785 (1988).

[6] A. Liebsch, Theory of photoemission from localized adsorbate levels, Physical Review B **13**, 544 (1976).

[7] T. Fujikawa and H. Arai, Many-body theory of core-level photoemission by Keldysh Green's functions, Journal of Electron Spectroscopy and Related Phenomena **123**, 19 (2002).

[8] S. Hasegawa, S. Tanaka, Y. Yamashita, H. Inokuchi, H. Fujimoto, K. Kamiya, K. Seki, and N. Ueno, Molecular orientation in thin films of bis(1,2,5-thiadiazolo)-p-quinobis(1,3-dithiole) on graphite studied by angle-resolved photoelectron spectroscopy, Physical Review B **48**, 2596 (1993).